Article

Carbon Sources and the Graphitization of Carbonaceous Matter in Precambrian Rocks of the Keivy Terrane (Kola Peninsula, Russia)

Ekaterina Fomina [1],* [ID]**, Evgeniy Kozlov [1]** [ID]**, Kirill Lokhov [2], Olga Lokhova [3] and Vladimir Bocharov [4]** [ID]

[1] Geological Institute, Kola Science Centre, Russian Academy of Sciences, 14, Fersmana Street, 184209 Apatity, Russia; kozlov_e.n@mail.ru

[2] Institute of Earth Sciences, Saint-Petersburg State University, 7/9, Universitetskaya Emb., 199034 St. Petersburg, Russia; k.lokhov@spbu.ru

[3] Institute for the History of Material Culture, Russian Academy of Sciences, 18, Dvortsovaya Emb., 191186 St. Petersburg, Russia; olga.lohova@yandex.ru

[4] Resource Center for Geo-Environmental Research and Modeling (GEOMODEL), Saint-Petersburg State University, 1, Ulyanovskaya Street, 198504 St. Petersburg, Russia; bocharov@molsp.phys.spbu.ru

* Correspondence: fomina_e.n@mail.ru; Tel.: +7-921-276-2996

check for updates

Abstract: The Precambrian rocks of the Keivy Terrane reveal five types of carbonaceous matter (CM): Fine-grained, flaky, nest, vein, and spherulitic. These types differ in their distribution character, carbon isotope composition, and graphitization temperatures calculated by the Raman spectra of carbonaceous material (RSCM) geothermometry. Supracrustal rocks of the Keivy Terrane contain extremely isotopically light ($\delta^{13}C_{PDB} = -43 \pm 3‰$) carbon. Presumably, its source was a methane–aqueous fluid. According to temperature calculations, this carbon matter and the host strata underwent at least two stages of metamorphism in the west of the Keivy Terrane and one stage in the east. The CM isotope signatures of several samples of kyanite schists ($\delta^{13}C_{PDB} = -33 \pm 5‰$) are close to those of oils and oil source rocks, and they indicate an additional carbon reservoir. Thus, in the Keivy territory, an oil-and-gas bearing basin has existed. Heavy carbon ($\delta^{13}C_{PDB} = -8 \pm 3‰$) precipitated from an aqueous CO_2-rich fluid is derived from either the lower crust or the mantle. This fluid probably migrated from the Keivy alkaline granites into the surrounding rocks previously enriched with "methanogenic" carbon.

Keywords: graphitization; carbon isotopes; RSCM geothermometry; polyphase metamorphism; alkaline granites; Precambrian; Kola Peninsula; graphite

1. Introduction

The Keivy Terrane of the Archean Kola Province, located in the northeast of the Baltic Shield, is a unique object for studying carbonaceous matter (CM). Different morphologies of CM are present in variable quantities in gneisses, amphibolites, quartzites, and schists of the Keivy and Tundra series [1]. The aluminous metapelites of the Keivy series (predominantly kyanite schists) are rich in carbon (0.1–2.3 wt % on average) [1–3]. These rocks are exposed over a wide area (Figure 1) of about 200 km in length and from several hundred meters to 10–14 km in width in the central part of the Keivy Terrane, as well as several smaller bands and lenses in its eastern and southern parts [3]. The rocks are considered to have originated from sediments that accumulated in a shallow water basin in a stable tectonic setting [1,2]. Keivy series schists are metamorphosed unequally. According to References [4–6], most of the stratum was metamorphosed under amphibolite facies conditions at

T = 450–560 °C and P = 4–5.3 kbar. In the central part of the Keivy Terrane (mostly in kyanite schists), metamorphism increased either to T = 550–600 °C and P = 6–6.5 kbar [5], or to T = 540–620 °C and P = 5.2–6 kbar [7]. In the east, temperatures were reduced to T < 500 °C (epidote–amphibolite facies, the pressure is not specified) [4,6]. Within the zone of influence of the alkaline granites (the western part of the Terrane), metamorphism proceeded under the conditions of kyanite–sillimanite subfacies of amphibolite facies at T = 550–650 °C and P < 4 kbar [4]. Thermodynamic constructions suggest several stages of metamorphism [5], but their numbers, ages, and correspondence to geodynamic events vary between authors [6]. The age of the metapelites is also debatable. Some authors believe that they are Archean [3,6,8–10], while others state that they are Paleoproterozoic [11,12]. However, reliable dating of these rocks has not been performed. In this article, we discuss previous and new data on CM, which abounds in the Keivy metapelites as scattered fine particles and larger intergranular flakes.
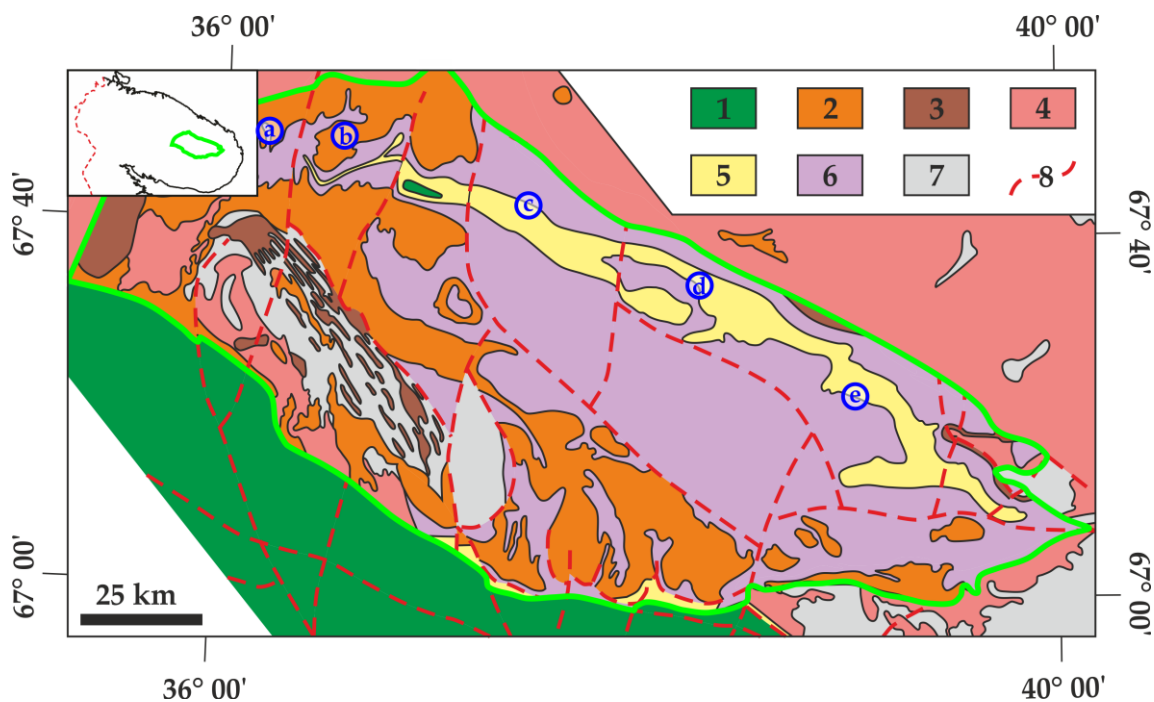
Figure 1. Geological scheme of the Keivy Terrane compiled on the basis of the 1:500,000 Geological Map of the Kola Region (simplified after Reference [13]), showing sampling locations (letters in blue circles): (**a**)—Makzabak (sillimanite schists); (**b**)—Rova (quartzolites); (**c**)—Tyapshmanyuk (kyanite schists); (**d**)—Shuururta (kyanite schists); (**e**)—Igiurta (kyanite schists). Legend: 1—mafic and ultramafic rocks, PR1; 2—Keivy alkaline granite complex, AR2; 3—gabbroids, AR2; 4—granitoids of normal alkalinity (undivided), AR2; 5—Keivy series aluminous schists, AR2; 6—Tundra series rocks (acidic, medium, basic metavolcanics, mica parashists), AR2; 7—gneisses and amphibolites of Kola series (basement complex), AR; 8—faults. The green line delineates the boundaries of the Keivy Terrane. The inset shows the position of the Keivy Terrane within the Kola Peninsula.

We present the first data on CM from alkaline granites of the Keivy Terrane. The Keivy alkaline granite complex has an age of 2.67–2.65 Ga [14–16] and it occupies an area of more than 2500 km^2 [17]. Due to the poor exposure of the contact zones, the relationship to the surrounding rocks is not clear. This gives rise to contradictory interpretations. Some authors suggested a metasomatic or rheomorphic genesis of granites ([11] and references therein). Others describe the intrusion of granitic magma either into formations of the same tectonomagmatic system [18] or into previously metamorphosed rocks [3,17]. These rocks are the world's oldest rare-metal anorogenic granites [15,16,19]. In the contact zones between the alkaline granites and the metamorphic rocks, as well as in the internal part of the granitic intrusions, pegmatites and quartzolites are common. Following [20,21], the term "quartzolite"

is used for a pegmatitic or hydrothermal rock that is primarily composed of quartz (> 60 vol %). The available geochronological estimates imply the possibility of the diachronous formation of pegmatites and quartzolites: The first formation stage was syngenetic to granites [16,20,22], and the second one occurred 1.6–1.7 Ga ago during the regressive stage of the Svecofennian metamorphic event [21,23]. The formation temperature of these rocks is about 400 °C [5]. The CM studied forms spherulites in quartzolite veins and lenses in the inner part of the Keivy alkaline granite complex.

Additionally, we studied large clusters of CM from the sillimanite schists, preserved in the west of the Keivy Terrane, about 100 m from the granites. The spatial proximity of the latter, as well as the structural and geochemical peculiarities of the sillimanite schists, allows for their formation to be related to the metamorphic–metasomatic processing of metapelites ([2,3] and references therein). CM forms nests from 5 to 10 cm in diameter, and veins from 0.2 to 2 cm in thickness in these rocks, which was explained to be a result of the assimilation and recrystallization of the initial metapelitic CM under the contact influence of granites [2,3].

Different CM morphologies occur in metamorphic rocks, magmatic rocks and metasomatic rocks, throughout the vast territory of the Keivy Terrane [1–3]. This makes the carbonaceous matter a witness of various geological events that occurred during the Precambrian era within the Keivy Terrane. CM morphology, the nature of its distribution, and its relationships with associated minerals play a highly informative role in the study of its precursors, and of the conditions for the transformation of host rocks during various metamorphic–metasomatic processes. This is due to the low CM mobility in rocks, and the peculiarity of its internal structure, which sensitively reflects peak crystallization conditions, remaining irreversible in the course of further retrograde transformations [2,24–26]. Geothermometry based on the Raman spectra of carbonaceous material (RSCM) was invented for different types of rocks [26–29]. This technique has been successfully used to estimate the peak temperatures of both regional and contact metamorphism [30–35]. According to Reference [36], it works even in the case of polymetamorphic complexes. Since the $^{13}C/^{12}C$ ratios of the main carbon reservoirs are contrasting [37–39], the carbon isotope characteristics of CM also provide valuable information on the nature of carbon in rocks.

In this paper, we report data from the Keivy Terrane CM, obtained by petrographic and mineralogical investigations, Raman spectroscopy, and carbon isotope analysis. Our study aims to characterize the main sources of carbon in the Keivy rocks, as well as to clarify controversial issues on the evolution of the Keivy Terrane, using CM as an indicator of peak thermal events. The results of this study are valuable, both for the understanding of the regional geology of the Kola Peninsula, and for a deeper understanding of crustal processes of the Precambrian period.

2. Materials and Methods

2.1. Samples

We investigated three rock species comprising all of the CM morphotypes currently known in the Keivy Terrane. To obtain the characteristics of the CM, we selected samples from five formations (Figure 1) that were geographically distant from each other: (1) CM-bearing quartzolites from the Keivy alkaline granite complex; (2) sillimanite schists near the contact with this massif; and (3) kyanite schists from three different areas (the Tyapshmanyuk, Shuururta, and Igiurta areas).

CM-bearing quartzolites (Figure 2a) were selected from a lens with an area of 10×20 m in the Rova locality in the western part of the Keivy alkaline granite complex. They represent a massive, coarse-grained rock of milky-white color, primarily composed of quartz (more than 90 vol %). Minor minerals were astrophyllite, arfvedsonite, and riebeckite, and accessory phases were titanite, pyrochlore, galena, and cassiterite. Sixteen samples of this rock were analyzed.
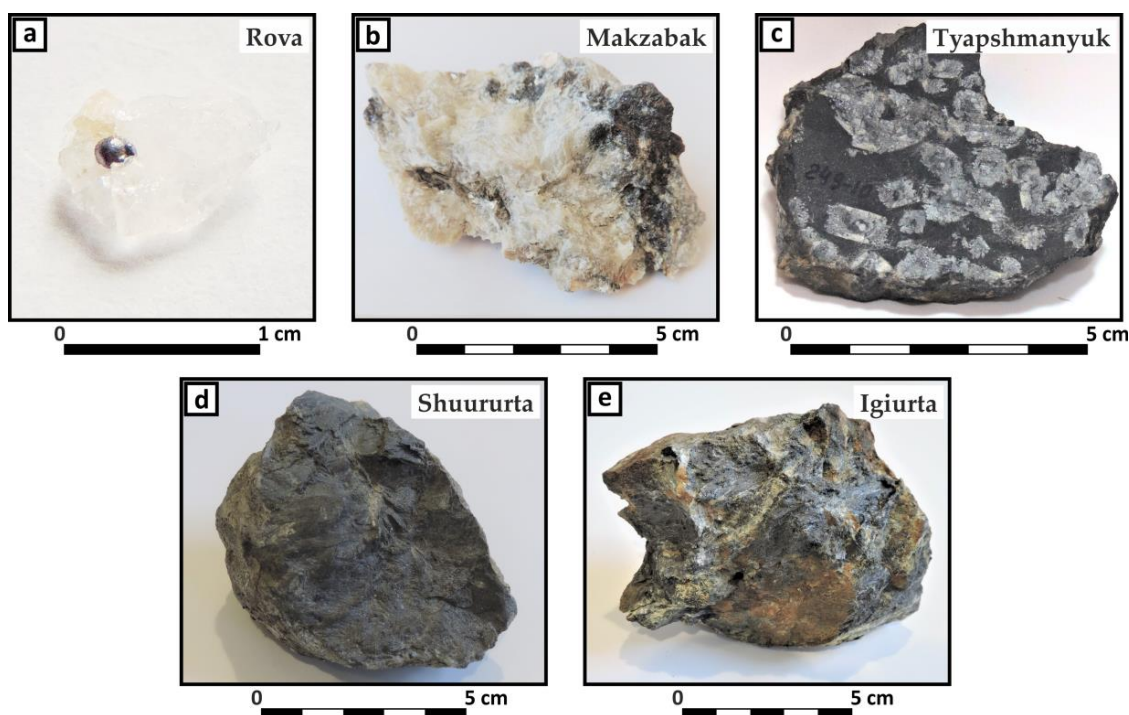
Figure 2. Studied carbonaceous matter (CM)-bearing rocks: (**a**) Quartzolite from the Keivy alkaline granite complex (the Rova area), (**b**) sillimanite schist, selected near the contact with this complex (the Makzabak area), and kyanite schists from (**c**) the Tyapshmanyuk, (**d**) the Shuururta and (**e**) the Igiurta areas.

Sillimanite schists (Figure 2b) crop out only in the west of the Keivy Terrane. We selected them from the Makzabak area, where they formed narrow strips and lenses (up to 20 × 300 m) in the enclosing mica and mica–garnet schists, at about 100 m from the contact to the alkaline granites. The major and secondary minerals of the sillimanite schists are (in varying amounts) sillimanite, staurolite, kyanite (locally), muscovite, margarite, quartz, chloritoid, CM, ilmenite, Nb-rutile, and apatite. Monazite, corundum, zircon, xenotime, and fergusonite occurred sporadically. The sheet silicates are often substituted by berthierine. Sillimanite schists are structurally highly heterogeneous; therefore, we selected 25 samples.

Kyanite schists were selected with eight samples from the Tyapshmanyuk mountain (Figure 2c) and 23 samples from Shuururta mountain (Figure 2d) of the central Keivy region, as well as 12 samples from the Igiurta mountain (Figure 2e) of the eastern Keivy region. These schists vary in sizes, orientations, and proportions of minerals; however, in general, the set of rock-forming minerals was constant. The main minerals are kyanite and quartz, and the minor ones are muscovite, plagioclase, staurolite, and CM.

2.2. Analytical Methods

Mineralogical and petrographic investigations of thin sections and polished thin sections in transmitted and reflected light were carried out by using an Axioplan 2 Imaging optical microscope (Carl Zeiss, Oberkochen, Germany). The morphology and structure of the CM-spherulites from quartzolites were additionally inspected by using contrasting backscattered electron (BSE) images obtained with a Hitachi S-3400N scanning electron microscope (the "Geomodel" RC SPbSU, St. Petersburg, Russia).

Carbon isotope analyses were conducted on an IRMC Delta V (Thermo Finnigan, San Jose, CA, USA) mass spectrometer at the Institute for the History of Material Culture of RAS (St. Petersburg). The samples were mechanically divided into pieces, each maximally enriched with one of the CM
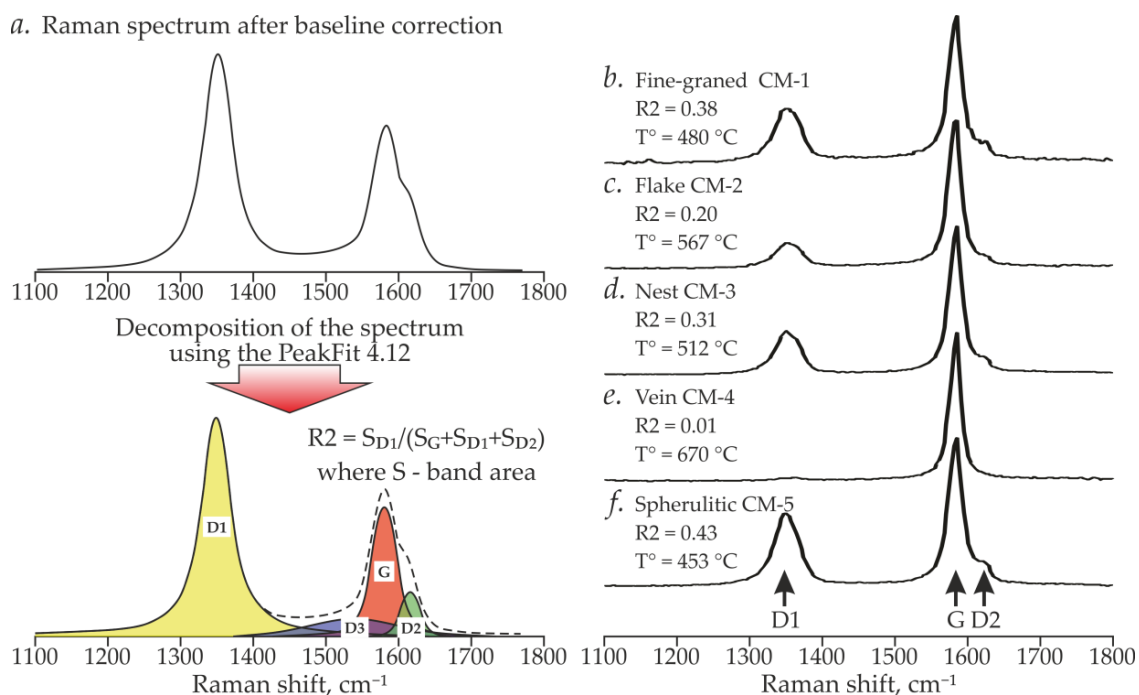
morphologies. Crushed samples of about 2 g in weight were subjected to chemical treatment with hydrochloric acid, with the addition of ammonium fluoride to dissolve the carbonate and silicate components. The extraction of the substance into the inlet system was initiated by combustion, i.e., transferring carbon to the CO_2 state. The instrumental error in determining the carbon isotopic composition did not exceed $\pm$ 0.05% (95% confidence interval). To validate the data and to exclude the instrument error, representative samples of each rock type from each object were additionally analyzed by using the Finnigan MAT Delta instrument in a dual inlet mode at the Institute of Geology and Mineralogy, SB RAS (Novosibirsk, Russia). The procedure of the carbon isotope analysis applied in the present study was analogous to that described in Reference [40].

In order to conduct interlaboratory verification, the collection of Raman spectra was carried out in two laboratories. Part of the data was obtained at the Institute of Geology of the KSC RAS with a Nicolet Almega XP (Thermo Scientific, Waltham, MA, USA) dispersive spectrometer equipped with an Olympus BX41 confocal microscope (Olympus Corporation, Tokyo, Japan) for navigation, using 50$\times$ and 100$\times$ objectives. An exciting He-Ne laser with a wavelength of 532 nm was used; the exposure time ranged from 4 to 30 s, and the number of repetitions was 2–30. Another part of the data was obtained at the "Geomodel" RC of the SPbSU Scientific Park (St. Petersburg) with a HORIBA Jobin-Yvon LabRam HR800 laser Raman spectrometer (Horiba, Ltd., Kyoto, Japan) equipped with an Olympus confocal microscope (100$\times$ objective lens, Olympus Corporation, Tokyo, Japan). The Raman scattering signal was excited by an Ar^+ laser (514.5 nm) with an acquisition time of 4–10 s, and with 10–15 repetitions. In both laboratories, the calibration was performed by using the Raman line of silicon at 521 cm^{-1}. The limit of the spectral resolution was about 2 cm^{-1}. The final laser power did not exceed 3 mW.

Polishing can damage the CM structure [41,42], and researchers often study CM beneath the surface of transparent adjacent grains [26,42,43]. Not all types of the studied CM were available for this method. The last polishing steps with an abrasive size less than 1 μm have the greatest impact on the CM structure [42,44]. In this study, uncoated samples polished by a monocrystalline diamond slurry with a grain size of 3 μm were used. The duration of polishing did not exceed 5 min. However, some influence of polishing on the CM structure could reduce the actual values of the graphitization temperatures. Where possible, the polarized laser beam was set to be perpendicular to the mean CM *c*-axis, which maximizes the Raman signal. The spectra of the neighboring mineral phases were also collected.

2.3. Raman Spectra Processing

Spectral decomposition (Figure 3) and the determination of the peak position, band area (*A*), peak width (*FWHM*), and band intensity (*I*) were performed using the PeakFit 4.12 software (Systat Software GmbH, Erkrath, Germany). Peaks were approximated by the Voigt function. The decomposition was based on the presence of peaks in the spectrum of natural CM, with up to 8–9 peaks [26,27,41]. According to this concept, in the first-order region (1100–1800 cm^{-1}), graphite with a perfect crystal structure exhibits only one sharp peak at ~1580 cm^{-1} (the so-called "G band"), corresponding to planar vibrations of carbon atoms in the structure. In the spectrum of less ordered CM with defects in graphene layers, additional first-order peaks appear at ~1350 cm^{-1} and ~1620 cm^{-1} (the D1 and D2 bands, respectively). In some cases, low-intensity bands that are especially wide in a poorly ordered amorphous matter, are also observed at about 1400–1500 cm^{-1} (D3) and 1100–1200 cm^{-1} (D4). As the degree of crystallinity increases, the relative intensities and areas of the D-peaks decrease, and the weak lines disappear [43]. An indicator of the CM ordering degree is the L*a* value (the in-plane crystallite size), which is calculated through the relative intensity ratio of the D1 and G bands [41,45]. The intensity-based R1 = I_{D1}/I_G ratio and area-based R2 = $A_{D1}/(A_G + A_{D1} + A_{D2})$ ratio are also used as sensitive parameters to describe the structural order of CM [26,29]. Peaks from the second-order region (2200–3400 cm^{-1}) located near 2400, 2700, 2900, and 3300 cm^{-1} are regarded as overtones or combination scattering [43].

a. Raman spectrum after baseline correction

Decomposition of the spectrum using the PeakFit 4.12

$R2 = S_{D1}/(S_G+S_{D1}+S_{D2})$
where S - band area

b. Fine-graned CM-1
R2 = 0.38
T° = 480 °C

c. Flake CM-2
R2 = 0.20
T° = 567 °C

d. Nest CM-3
R2 = 0.31
T° = 512 °C

e. Vein CM-4
R2 = 0.01
T° = 670 °C

f. Spherulitic CM-5
R2 = 0.43
T° = 453 °C

Figure 3. (**a**) Schematic decomposition diagram of CM Raman spectrum in the first-order region (1100–1800 cm⁻¹) and (**b**–**f**) characteristic spectra (in the same region) of different CM morphologies from the studied rocks of the Keivy Terrane.

The graphitization temperature of CM was assessed by an RSCM geothermometer, calibrated (1) for a 514.5 nm laser for regional metamorphism [26], and those calibrated for a 532-nm laser [27] (2) for contact and (3) for regional metamorphism. The first RSCM geothermometer has an absolute precision of ±50 °C, while in the last two calibrations, it is of ±30 °C. The calculations of temperatures by the first geothermometer are closest to the average values of the three indicated thermometers. The second geothermometer yielded 5–10 °C higher, and the third geothermometer yielded 10–15 °C lower temperatures. Hereafter, the results of only the calculations by the first geothermometer are presented. This geothermometer is valid for the temperature range of 330–650 °C [26].

3. Results

3.1. Morphology of Carbonaceous Matter

Five morphological types of CM were found (in order of prevalence): Dispersed fine particles (hereafter fine-grained CM), flakes, irregular aggregates (hereafter "nests" or "nest CM"), veins, and spherulites (Figures 2 and 4).

The fine-grained carbonaceous (CM-1) is presented in all studied schists (Figure 4a,b). This form reached the highest concentrations in kyanite schists, coloring them gray to black (see Figure 2c–e). It is quite evenly dispersed in the rock matrix as tiny particles ranging in size from fractions of microns to three microns, and it was included in rock-forming silicates. Notably, the fine- and medium-grained areas of the schists tend to be enriched with CM-1 more than large silicate crystals.

Metapelites contain flaky carbonaceous matter (CM-2) in variable quantities, from a few microns to 0.05 mm in length, localized in the interstitial space, within schistosity, and/or along grain cracks (Figure 4c,d). In the kyanite schists, large kyanite paramorphoses are light, almost devoid of CM inclusions, and contain flaky CM along their edges, cracks, and interstities (see Figures 2c and 4c). The kyanite schists of the Igiurta mountain (east of the Keivy Terrane) does not contain this CM morphology, while CM-1 was ubiquitous therein.
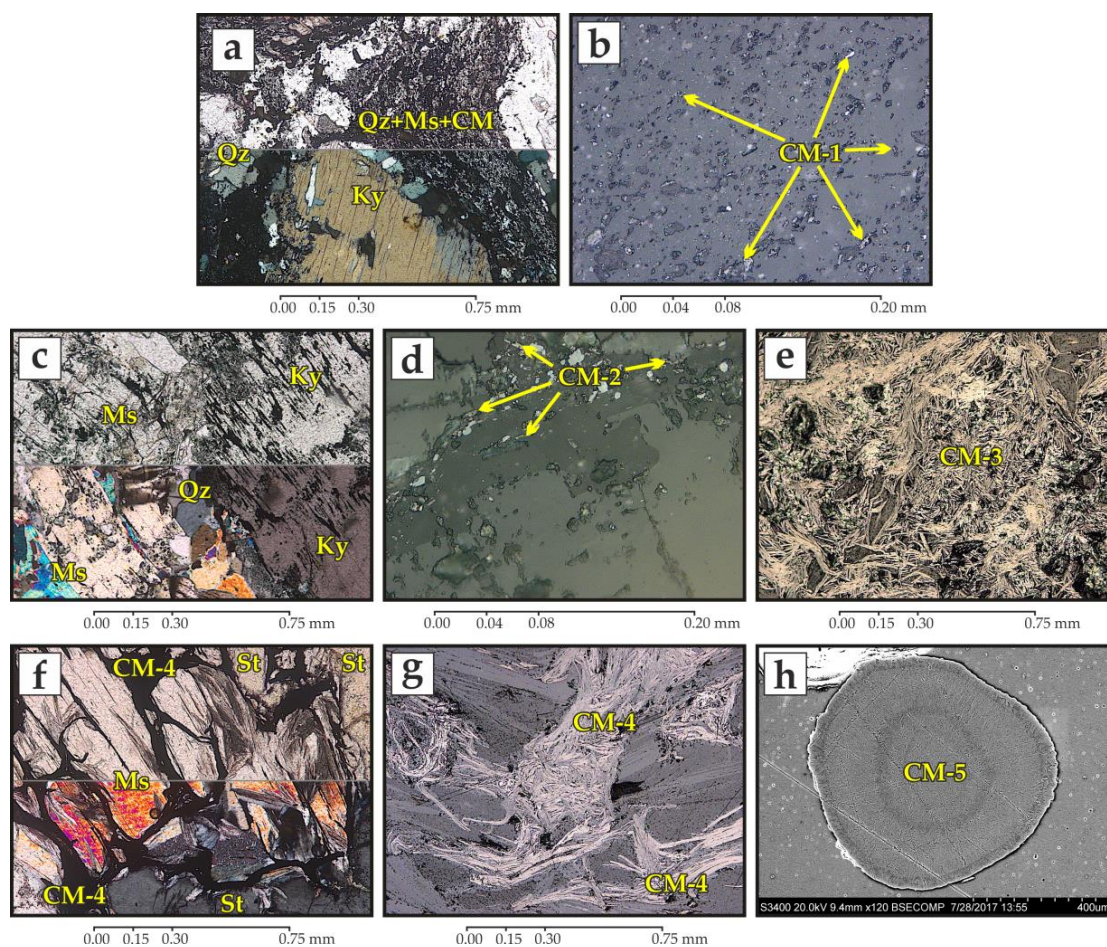
Figure 4. CM morphologies and their position in the studied rocks from the Keivy Terrane: (**a**) Section of a sample of kyanite schist with CM-bearing matrix and (**b**) morphology of fine-grained CM-1 therein; (**c**) interstitial distribution of flaky CM-2 in kyanite-muscovite segregations and (**d**) morphology of CM-2; (**e**) nest of CM-3; (**f**) muscovite-staurolite part of the sillimanite schist veined with CM-4 and (**g**) the morphology of the latter; (**h**) zoning in spherulitic CM-5. Images: (**h**) is a backscattered electron (BSE) photomicrograph; (**a**,**c**,**f**) are transmitted light photomicrographs (top—one polarizer, bottom—two polarizers); (**b**,**d**,**e**,**g**) are reflected light photomicrographs. Abbreviations: CM – carbonaceous matter (the numbers correspond to the morphologies, see explanations in the text); Ms—muscovite; Ky—kyanite; Qz—quartz; and St—staurolite.

Sillimanite schists contain four CM morphologies: In addition to CM-1 and CM-2, nest (CM-3) and vein (CM-4) varieties. CM-1 and CM-2 are sporadically present in staurolite grains and sillimanite fibrolites only. CM in these rocks has a dominantly "nest" morphology of up to 10 cm in width, distributed extremely unevenly. The nests are composed of aggregates of mid-sized sinuous flakes (CM-3) (Figure 4e).

Vein carbonaceous matter (CM-4) occurs exclusively in sillimanite schists. The thickness of the veins ranges from a few millimeters to 2 cm. They are composed of curved planks of CM, interspersed with rutile and ilmenite. Notably, CM-4 veins crosscut the main minerals in the rock, including staurolite (Figure 4f,g).

CM-5 from quartzolites located inside the alkaline granite massif occurrs exclusively as spherulites ranging in size from fractions of a millimeter to 5 mm. These spherulites are uneven, composed of dense aggregates, often zonal (Figure 4h), and distributed chaotically in the rock. Sometimes, intergrowths of several spherulites were observed. Spherulitic CM morphology has not been previously described in any rocks of the Keivy Terrane, although it is known in various geological objects [46–49].

3.2. Stable Carbon Isotope Data

The investigated CM exhibited significant differences in carbon isotope composition (Table 1).

Table 1. Carbon isotope composition of CM from the Keivy Terrane.

Sample	Locality	Long. (N)	Lat. (E)	Host Rock [1]	CM Type	n[2]	$\delta^{13}C_{PDB}$, ‰
K-162	Igiurta	67.36658	39.02185	Ky	CM-1	2	−33.3 . . . −38.2
K-163	Igiurta	67.36794	39.02407	Ky	CM-1	4	−41.3 . . . −45.8
K-164	Igiurta	67.36933	39.02696	Ky	CM-1	3	−41.4 . . . −45.9
K-165	Igiurta	67.37166	39.03104	Ky	CM-1	3	−45.2 . . . −46.8
Igiurta, kyanite schists, only CM-1, n = 12: Median −44.7‰, mean −43.1‰, SD 4.0‰							
249-10	Tyapshmanyuk [3]	67.72212	37.43463	Ky	CM-1 + CM-2	4	−43.4 . . . −44.5
250-10	Tyapshmanyuk [3]	67.72084	37.43778	Ky	CM-1 + CM-2	4	−43.7 . . . −44.8
Tyapshmanyuk, kyanite schists, CM-1 + CM-2 mix, n = 8: Median −44.2‰, mean −44.2‰, SD 0.5‰							
K-197	Shuururta	67.58354	38.21614	Ky	CM-1 + CM-2	2	−29.1 . . . −36.1
K-200	Shuururta	67.58362	38.22089	Ky	CM-1 + CM-2	2	−41.3 . . . −45.1
K-201	Shuururta	67.58420	38.22161	Ky	CM-1 + CM-2	4	−27.3 . . . −33.1
K-202	Shuururta	67.58534	38.22317	Ky	CM-1 + CM-2	3	−30.1 . . . −33.4
K-203	Shuururta	67.58634	38.22675	Ky	CM-1 + CM-2	2	−35.2 . . . −35.7
K-216	Shuururta	67.59379	38.28372	Ky	CM-1 + CM-2	3	−30.9 . . . −38.3
G2-14-2	Shuururta	67.53086	38.09548	Ky	CM-1 + CM-2	1	−37.7
G3-17-1	Shuururta	67.58487	38.22785	Ky	CM-1 + CM-2	1	−32.6
G3-17-2	Shuururta	67.58487	38.22785	Ky	CM-1 + CM-2	1	−33.2
G3-18-1	Shuururta	67.54943	38.27469	Ky	CM-1 + CM-2	1	−40.2
G3-21-1	Shuururta	67.55296	38.29061	Ky	CM-1 + CM-2	1	−37.8
G4-30-1	Shuururta	67.56740	38.08735	Ky	CM-1 + CM-2	1	−33.2
G4-31-1	Shuururta	67.56934	38.06529	Ky	CM-1 + CM-2	1	−34.5
Shuururta, kyanite schists, CM-1 + CM-2 mix, n = 23: Median −33.4‰, mean −34.3‰, SD 4.4‰							
F13028	Makzabak	67.84095	36.17565	Sill	CM-3 + CM-4	20	−14.2 . . . −22.6
Makzabak, sillimanite schists, CM-3 + CM-4 mix, n = 20: Median −17.4‰, mean −18.3‰, SD 1.7‰							
F13028	Makzabak	67.84095	36.17565	Sill	CM-4	2	−10.1 . . . −10.7
Makzabak, sillimanite schists, only CM-4, n = 2: Median −10.4‰, mean −10.4‰, SD 0.4‰							
F12026	Rova	67.83838	36.54107	Qz	CM-5	9	−5.6 . . . −9.1
Rova, quartzolites, CM-5, n = 9: Median −7.5‰, mean −7.4‰, SD 1.9‰							

[1] Hereafter: Ky—kyanite schists, Sill—sillimanite schists, Qz—quartzolites; [2] n—the number of analyses; [3] Coordinates of the samples from the Tyapshmanyuk area are taken from the map.

Isotope data of an inseparable mixture of fine-grained CM-1 and flaky CM-2 for kyanite schists of the Tyapshmanyuk mountain are homogeneous with $\delta^{13}C_{PDB}$ = −43.4‰ to −44.8‰. CM-1 from the Igiurta mountain shows an isotopic composition close to that of the CM from Tyapshmanyuk mountain, although it is more variable (from −41.3‰ to −46.8‰). For one sample, heavier values were obtained (−35.8 ± 2.5‰). Carbon isotope data for kyanite schists from Shuururta mountain, where CM-1 and CM-2 morphologies were found, are divided into two sets. Three analyses (from two samples) yielded a $\delta^{13}C_{PDB}$ value of −42.7 ± 2.5‰. In the other 20 analyses, values vary from −27.3‰ to −38.3‰, with the most values in a range of ±2.5‰ from a median of −33.2‰. Sillimanite schists of the Makzabak area contain several CM types. The range of $\delta^{13}C_{PDB}$ variations for the nest CM-3 (possibly contaminated by CM-4) is −14.2‰ to −22.6‰, with more than half of the analyses falling into the interval −17.4 ± 0.4‰. The carbon of the CM-4 veins is significantly heavier, with $\delta^{13}C_{PDB}$ values of −10.1 to −10.7‰. Spherulites from the Rova quartzolites contain the heaviest carbon, with $\delta^{13}C_{PDB}$ values of −5.6‰ to −9.1‰.

3.3. RSCM Temperature Estimates

The Raman spectra of all investigated CM types except for spherulites yield R2 ratio values of <0.40 (Table 2). This, according to Reference [50], indicates that the fine-grained CM-1, flaky CM-2, nest CM-3, and vein CM-4 correspond to graphite. The spherulitic CM-5 corresponds to semi-graphite.

Table 2. Summary of Raman spectra of carbonaceous material (RSCM) peak temperature determinations from CM-bearing rocks of the Keivy Terrane.

| Locality	Host Rock	CM Type	n	FWHM$_G$ (SD)	R1 (SD)	R2 (SD)	T (SD)	T* [R1*]	FWHM$_G$* Calc.
Igiurta	Ky	CM-1	18	18.6 (1.1)	0.30 (0.17)	0.36 (0.09)	480 (42)	522 [0.15]	19.3
Tyapshmanyuk	Ky	CM-1	10	22.3 (1.5)	0.29 (0.04)	0.32 (0.03)	501 (14)	510 [0.24]	22.5
Tyapshmanyuk	Ky	CM-2	6	20.7 (0.6)	0.18 (0.03)	0.21 (0.01)	549 (5)	552 [0.16]	19.5
Shuururta	Ky	CM-1	6	18.7 (2.0)	0.34 (0.23)	0.36 (0.12)	482 (51)	525 [0.17]	20.0
Shuururta	Ky	CM-2	8	17.1 (0.7)	0.12 (0.03)	0.19 (0.03)	557 (15)	564 [0.10]	16.8
Makzabak	Sill	CM-3	15	23.0 (1.2)	0.44 (0.16)	0.38 (0.07)	472 (32)	496 [0.23]	21.9
Makzabak	Sill	CM-4	7	20.3 (1.8)	0.10 (0.07)	0.13 (0.09)	582 (42)	636 [0.01]	14.1
Rova	Qz	CM-5	68	19.2 (1.7)	0.43 (0.08)	0.42 (0.04)	454 (18)	499 [0.25]	22.6

Note: R1, R2, and peak temperature values calculated using the calibration of [26]; SD—standard deviation; n—the number of analyses; FWHM$_G$—G band width at half-maximum; T*—peak temperature for the sample with R1*, where R1* (in square brackets) is the minimum R1 value for the corresponding sampling; FWHM$_G$* calc.—the value of G band width at half-maximum, calculated by the formula FWHM$_G$ = 14 + 35R1 [51] for R1*.

The peak-temperature ranges for the fine-grained CM-1 from the kyanite schists are (Figure 5):

- From 470 to 520 °C, with a mean value of 500 °C, for the samples of Tyapshmanyuk mountain;
- From 390 to 530 °C, with a mean value of 480°C, for the Shuururta mountain samples;
- From 390 to 520 °C, with a mean value of 480 °C, for the samples from the Igiurta mountain.

Raman spectra of flaky CM-2 indicate a higher structural order, and, consequently, the calculated temperature range is 540–560 °C for the Tyapshmanyuk mountain samples, and 540–590 °C for the Shuururta mountain samples.

The nest CM-3 from the sillimanite schists is characterized by a chaotic arrangement of CM grains. In this regard, the orientation of the laser beam perpendicular to the *c*-axis was hampered. The calculated temperatures range from 430 to 520 °C, with a mean value of 470 °C.
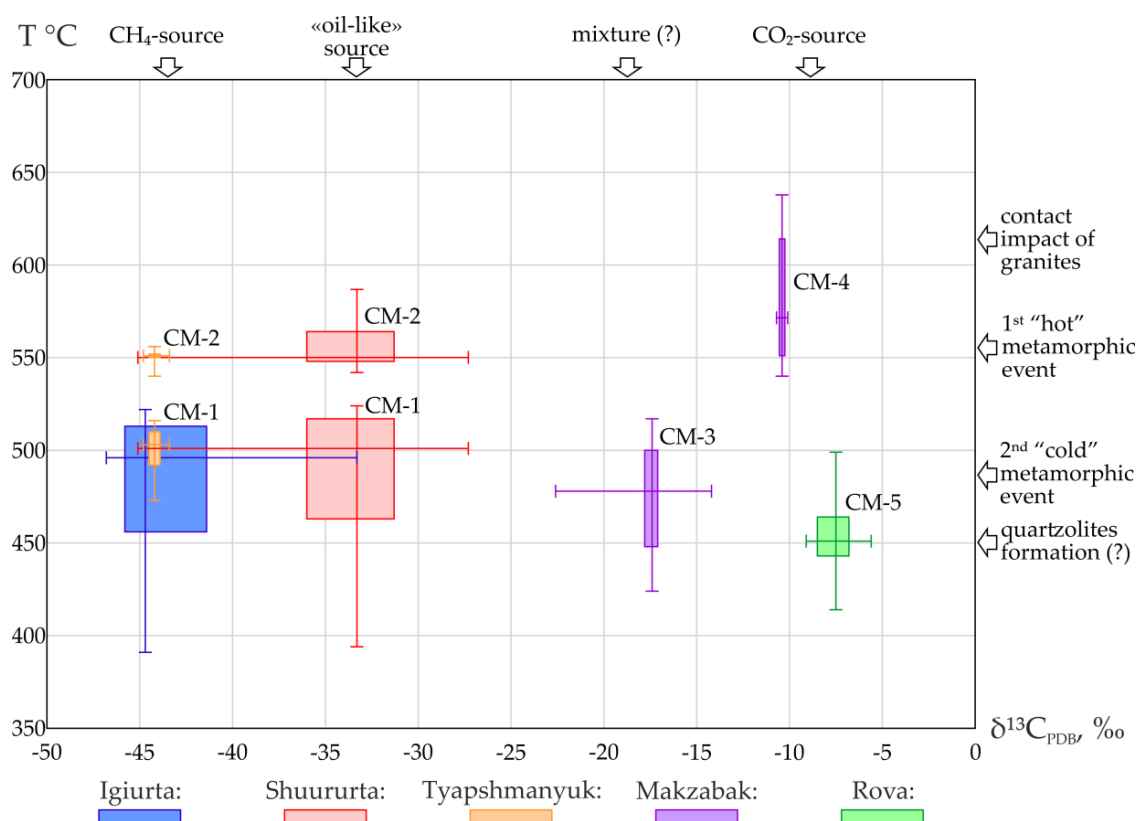
Figure 5. Variations in carbon isotope compositions ($\delta^{13}C_{PDB}$) and crystallization temperatures (T °C) of CM morphotypes (signed) from the rocks of the studied objects. Top marks the possible sources of carbon. To the right of the frame, the thermal mode of events during which CM crystallized is shown (the rationale for this data interpretation is discussed in Section 4). For the Shuururta and Tyapshmanyuk rocks, CM-1 and CM-2 were not amenable to separation, therefore the isotope characteristics of mixtures are displayed.

In the spectrum of the vein CM-4, the narrowest G peak was observed, and the disorder bands are very weak or completely absent. Its structure is the most well-ordered compared to the other morphologies [41]. The calculated peak temperatures are about 540–640 °C, with a mean value of 580 °C close to the upper limit of applicability of the geothermometer [26].

The lowest temperatures were obtained for spherulites. Notably, the zoning seen on the BSE photo is controlled by the variability in the ordering degree of the carbonaceous matter, which is reflected in their Raman spectra. The number of zones in the spherulites varied depending on their size. On average, the calculated temperature range for the CM-5 spherulites is about 410–500 °C, with a mean value of 450 °C. The temperatures calculated for CM-5 (and, possibly, CM-4) are suppositive (most likely minimal), since the crystallinity degrees of vein and magmatic CM are not clearly correlated with temperature [41,52,53].

To assess the RSCM results, it is necessary to evaluate the polishing effect on the obtained RS data. In Reference [51], it was shown that polishing increases the R1 ratio. On the contrary, G-band width at half-maximum (FWHM_G) parameter is polishing resistant and is related with the R1 value by the linear function of FWHM_G = 14 + 35R1 [51]. The measured R1 values of each of the eight groups of CM from the Keivy Terrane (see Table 2) vary widely (R1 in Table 2), which indicates the effect of polishing. The FWHM_G values within these groups are almost identical (FWHM_G in Table 2). This confirms the insensitivity of this parameter to polishing. We selected the Raman spectra of those samples in which CM was least affected by polishing. Those spectra have minimal R1 values (R1* in Table 2). An additional selection controller is the proximity of the individual FWHM_G values (FWHM_G* in Table 2) calculated by using R1* to the average FWHM_G values of the sampling. Comparison of temperatures

T* with average sampling temperatures (T) made it possible to evaluate deviations in estimates of peak temperatures. In CM-1, in CM-2, and in CM-3, the difference between T* and T is not large (20–40 °C), and the $FWHM_G$ and $FWHM_G$* are close. The results obtained are systematically lowered. The error is within the absolute precision of the geothermometer used [26]. Thus, the determined values correspond to the lower limit of the true peak temperatures. Notably, T* values are close to T measurements made by using the (3) geothermometer [27]. For CM-4 and CM-5, the differences between T* and T are higher, and the $FWHM_G$ and $FWHM_G$* differ noticeably. Thus, the true peak temperatures of CM-4 and CM-5 should be considered to be higher, which is consistent with [53].

Statistical processing of the obtained peak temperatures is required for the reliable discrimination of the graphitization conditions. Based on the asymmetry of the "box-and-whiskers" and the length of the "whiskers" (Figure 5), we can assume a multiplicity of outliers, and the absence of a normal distribution of peak temperatures for most of the CM types. Therefore, robust nonparametric statistics (the median test, the Kruskal–Wallis test, the Kolmogorov–Smirnov test, and the Mann–Whitney U test) were used [54–57]. All tests were performed for the $p = 0.05$ confidence interval.

A comparison of the CM-1 and CM-2 peak temperatures from three kyanite schist localities shows that CM-1 and CM-2 do not belong to a single data sample, as they have different medians and distributions. Statistical tests for CM-2 from different areas reveal a high probability of their belonging to a single data sample, with a general median of 560 °C (in different tests, *p* vary from 0.6 to 0.8). Statistically, vein CM-4 from sillimanite schists can also be part of this data sample (*p* from 0.2 to 0.4). Similarly, CM-1 from different localities of kyanite schists are parts of a single data sample, with a general median of 500 °C (*p* from 0.8 to 1.0). The nest CM-3 from sillimanite schists can also be considered to be part of this data sample (*p* from 0.3 to 0.4). Only CM-3 is statistically close to spherulitic CM-5 from quartzolites. The median of the combined CM-3 + CM-5 data sample is 450 °C. However, the probability that these two CM types belong to a single data sample is close to the selected significance level (*p* from 0.1 to 0.2).

4. Discussion

In rocks of the Keivy Terrane, five CM types, with different morphologies, structural positions, crystallization temperatures, and carbon isotope signatures are present. The largest amounts of carbon in the Keivy Terrane are formed as fine-grained (CM-1) and flaky (CM-2) matter. In the mid-1970s, the first carbon isotope data for CM from kyanite schists from Shuururta mountain (about 35‰) were published [1]. Based on this, all carbon in the Keivy Terrane was henceforth considered as a product of the metamorphism of sedimentary biogenic matter. An extremely isotopically light carbon ($\delta^{13}C_{PDB}$ from –42‰ to –47‰) was detected in high-Al metamorphic schists and metasomatic kyanite rocks from shear zones of the Keivy Terrane (Vorgel'urta and Manyuk areas) [58].

Light CM ($\delta^{13}C_{PDB}$ = –43.5 ± 3.3‰) is a characteristic for all kyanite schists of the study area. Rocks traced in a zone of about 200 km in length have this isotopic signature. Following [58], the source of carbon depleted in the ^{13}C could be an aqueous-methane fluid from sedimentary rocks with organic compounds. This is consistent with the data on fluid inclusions in kyanite rocks, which contain CO_2 and solutions of calcium and sodium chlorides, methane and "heavier" hydrocarbons [58]. Abiogenic methane from the Fennoscandian, Canadian, and African Shields has similar isotope characteristics [59–62]. However, according to Reference [63], "as the thermal stress on carbon complexes increases, more ^{12}C–^{13}C bonds are broken and the gas becomes isotopically heavier". Methane, a precursor of CM, should have been isotopically lighter [39]. Such signatures are then beyond the limits of variations in the isotopic composition of abiogenic methane ([64] and references therein).

Our investigation confirms the existence of CM with an isotopic composition of $\delta^{13}C_{PDB}$ –32.8 ± 5.5‰, along with extremely isotopically light CM ($\delta^{13}C_{PDB}$ = –43.5 ± 3.3‰) in kyanite schists of the Shuururta mountain. Moreover, one probe from the Igiurta mountain yielded heavier ($\delta^{13}C_{PDB}$ –35.8 ± 2.5‰) values. This indicates the probability of carbon assimilation from an additional

reservoir that was more highly enriched in the ^{13}C isotope. Similar isotopic signatures are seen in oils and oil source rocks [39,65,66]. In this light, the recent discovery of forms externally resembling nanobacteria in the schist samples from Shuururta mountain is of interest [67]. It is possible that these organisms contributed to the carbon isotope signatures of some parts of metasedimentary strata in this area. However, taking into account rather large variations in the isotopic composition of the abiogenic gas [59], this CM could also be of abiogenic origin. Nevertheless, the coexistence of isotopic signatures resembling those of natural gases and oils allows us to assume the existence of a Precambrian oil-and-gas-bearing basin within a considerable area of the Keivy Terrane. This hypothesis is supported by recent geodynamic reconstructions, according to which the Keivy Terrane ("domain") could have been a "median massif" during the Neoarchean period, which is often characterized by the presence of hydrocarbon deposits [68].

The isotopically heavy ($\delta^{13}C_{PDB}$ = –7.4 ± 1.8‰) carbon of the CM-5 spherulites from the intragranite quartzolites of the Keivy alkaline granite complex could be derived either by CO_2 assimilation from lower-crustal fluids or from CO_2-rich mantle fluids [37,69]. A similar carbon isotopic composition ($\delta^{13}C_{PDB}$ = –10.4 ± 0.3‰) was found in vein CM-4. This indicates the kinship of the CM-4 and CM-5 precursors. Previously, mantle-derived CM was not detected in the Keivy Terrane. One of the important results of our study is the discovery of at least three isotopically contrasting carbon sources.

According to the isotope data, the carbon of CM-3 is intermediate between "methanogenic" and "mantle" ($\delta^{13}C_{PDB}$ = –18.4 ± 4.5‰). This is possibly a product of fluid remobilization of extremely light carbon that was dynamically enriched in ^{13}C isotope during its migration. The second scenario is that carbon precipitated from a multicomponent mixture of CH_4-rich and CO_2-rich fluids from the above sources. Alternatively, these isotope characteristics could be the result of mixing between the isotopically light and heavy forms of carbon matter [70,71].

The results of RSCM thermometry demonstrate statistically significant differences in the peak temperatures of CM-1 and CM-2. Graphitization is a progressive, irreversible transformation [24,25,41]. Therefore, the coexisting CM-1 and CM-2 in kyanite schists, and CM-3 and CM-4 in sillimanite schists with different graphitization temperatures are indicators of polymetamorphic events. This is in good agreement with the conclusions on the multi-stage regional metamorphism of supracrustal formations of the Keivy Terrane [5,6] The described coexistence is possible only if the second event was lower in temperature. Otherwise, the graphitization temperatures would be the same for both CM types, and they would correspond to the maximum thermal effect [25].

Thus, the earliest metamorphic event recorded in the CM of the kyanite schists was the peak metamorphism (about 550 °C). The obtained values are close to the termobarometrical estimates of the kyanite schist formation [4,7]. CM-4 peak temperatures from sillimanite schists are statistically similar to those of CM-2 flakes. This suggests graphitization by a single event. The carbon isotope signatures of CM-4 and its morphology indicate fluid transportation of a parental compound of C (probably, CO_2) from the endogenous (granitic) source. The fluid nature of vein CM-4 does not permit the unequivocal acceptance of its thermometric estimates (> 580 °C) [41,52]. However, they are close to the estimates for metamorphic conditions of sillimanite schists (550–650 °C) [5]. Structural relationships of the vein CM-4 with sillimanite, staurolite, and muscovite (namely, its crosscutting of the indicated minerals) suggest that CM-4 was generated later than the minerals of metamorphic association of host rocks. Hence, supracrustal rocks of the Keivy Terrane underwent metamorphism either prior to the intrusion of a granitic melt ("zero metamorphic event"), or contemporaneously with this intrusion (2.67–2.65 Ga). The latter assumption supports the idea of the formation of sillimanite schists under the thermal influence of alkaline granite intrusions [3].

The CM-2 and CM-4 peak temperatures are the same. Apparently, an early event involved the regional heating of the rocks of the Keivy Terrane during the large-scale granitic intrusion in the Archean. The maximum thermal exposure was manifested around the contacts of the granitic massifs, which is fixed at the peak temperatures of CM-4.

No signs of the peak temperature effect were found in kyanite schists of the Igiurta mountain. This suggests a decrease in the intensity of the first (hot) metamorphic event from the northwest to the east of the Keivy Terrane, which confirms the previous thermobarometric estimates [4,5].

The second (regressive) event induced the graphitization of CM-1 in kyanite schists and CM-3 in sillimanite schists. Its peak temperatures are about 500 °C, and the impact is traced throughout the Keivy Terrane.

Considering the obtained temperature estimates, the CM-5 spherulites may have crystallized at the final formation stage of the granite massif. This is consistent with quartzolite formation temperature estimates [5], and the idea that the host quartzolites are the end-members of the granitic magma fractionation formed by residual fluid-saturated Si-rich melts [20,22]. The graphitization temperatures of spherulites (about 450 °C) slightly exceeded those that were obtained by classical thermobarogeochemical methods for quartzolites (about 400 °C) [5]. Possibly, this is caused by the influence of the regressive ("cold") regional metamorphism.

5. Conclusions

1. The extremely light ($\delta^{13}C_{PDB}$ = –40.2‰ to −46.8‰) carbonaceous matter characterizes the rocks from the northwest to the east of the Keivy Terrane.
2. In the kyanite schists of the Shuururta mountain and the Igiurta mountain, along with extremely isotopically light CM, that with a carbon isotope composition of about –33‰ $\delta^{13}C_{PDB}$ is widespread. This denotes the existence of an additional carbon reservoir.
3. Within the Keivy Terrane, CM with isotopically heavy carbon ($\delta^{13}C_{PDB}$ = −5.6‰ to −10.7‰) occurs both in quartzolites from alkaline granites, and in the sillimanite, schists surrounding the latter.
4. CM graphitization in kyanite schists most likely occurred in two stages of regional metamorphism, the peak event and the regressive event, respectively. Peak temperatures of the CM graphitized are maximal in sillimanite schists surrounding alkaline granites in the northwest of the Keivy Terrane (> 580 °C). Those in the kyanite schists from the central part of the Terrane are lower (~ 550 °C). In CM from the east of the Keivy Terrane, no evidence of this peak metamorphic event was found. The mineral associations of the sillimanite and kyanite rocks, corresponding to amphibolite facies, reflect this early hot event. The obtained data suggest a relationship between this event and the regional heating induced by the intrusion of alkaline granite magmas in the Archaean period.

The second metamorphic event affected all supracrustal rocks of the Keivy Terrane. It proceeded at temperatures of about 500 °C. The traces of this event were recorded in the mineral associations and CM of kyanite schists of the eastern part of the Keivy Terrane, metamorphosed under epidote–amphibolite facies conditions.

References

1. Sidorenko, S.A.; Sidorenko, A.V. *Organic Matter in the Precambrian Sedimentary-Metamorphic Rocks*; Nauka: Moskow, Russia, 1975. (In Russian)

2. Melezhik, V.A.; Basalayev, A.A.; Predovskiy, A.A.; Balabonin, N.L.; Bolotov, V.I.; Pavlova, M.A.; Gavrilenko, B.V.; Abzalov, M.Z. *Carbon Deposits of the Early Stages of the Earth's Development (Geochemistry and Accumulation Conditions on the Baltic Shield)*; Zhukov, R.A., Ed.; Nauka: Leningrad, Russia, 1988. (In Russian)

3. Bel'kov, I.V. *Kyanite Schists of the Keivy Suite*; Tochilin, M.S., Ed.; Academy of Sciences USSR: Leningrad, Russia, 1963. (In Russian)

4. Petrov, V.P.; Belyaev, O.A.; Voloshina, Z.M.; Bogdanova, M.N.; Ivliyev, A.I. *Metamorphism of Early Precambrian Supracrustal Complexes*; Zagorodniy, V.G., Ed.; Nauka: Leningrad, Russia, 1986. (In Russian)

5. Petrov, V.P.; Belyaev, O.A.; Voloshina, Z.M.; Balagansky, V.V.; Glazunkov, A.N.; Pozhilenko, V.I. *Endogenous Metamorphic Regimes of the Early Precambrian (Northeastern Part of the Baltic Shield)*; Mitrofanov, F.P., Ed.; Nauka: Leningrad, Russia, 1990. (In Russian)

6. *Early Precambrian of the Baltic Shield*; Glebovitskii, V.A. (Ed.) Nauka: St.-Petersburg, Russia, 2005. (In Russian)

7. Pindyurina, E.O.; Kol'tsov, A.B. Schists of Keiv metamorphic complex (Kola Peninsula): Mineral paragenesis and formation conditions. *Vestn. Spbsu* **2015**, *7*, 38–58. (In Russian with English Abs.)

8. Pushkarev, Y.D. *Megacycles in the Evolution of the Crust–Mantle System*; Nauka: Leningrad, Russia, 1990. (In Russian)

9. Radchenko, A.T.; Balaganskiy, V.V.; Basalaev, A.A.; Vinogradov, A.N.; Golionko, G.B.; Petrov, V.P.; Pozhilenko, V.I.; Radchenko, M.K. *Precambrian Tectonics of the Northeastern Part of the Baltic Shield (Explanatory Note for the 1:500,000 Geological Map)*; Mitrofanov, F.P., Ed.; Nauka: St.-Petersburg, Russia, 1992. (In Russian)

10. Bushmin, S.A.; Glebovitskii, V.A.; Presnyakov, S.L.; Savva, E.V.; Shcheglova, T.P. New data on the age (SHRIMP II) of protolith and paleoproterozoic transformations of the Archean Keivy terrain (Kola Peninsula). *Dokl. Earth Sci.* **2011**, *438*, 661–665. [CrossRef]

11. Mints, M.V. 3. Neoarchean intracontinental areas of sedimentation, magmatism, and high-temperature metamorphism (hot regions) in eastern Fennoscandia. In *East European Craton: Early Precambrian History and 3D Models of Deep Crustal Structure*; Mints, M.V., Konilov, A.N., Philippova, I.B., Zlobin, V.L., Babayants, P.S., Belousova, E.A., Blokh, Y.I., Bogina, M.M., Bush, W.A., Dokukin, P.A., et al., Eds.; Geological Society of America: Boulder, CO, USA, 2015; Volume 510, ISBN 9780813725109.

12. Fallick, A.E.; Hanski, E.J.; Kump, L.R.; Medvedev, P.V.; Melezhik, V.A.; Prave, A.R.; Svetov, S.A. The Palaeoproterozoic of Fennoscandia as context for the Fennoscandian Arctic Russia—Drilling Early Earth Project. In *The Early Palaeoproterozoic of Fennoscandia: Geological and Tectonic Settings // Reading the Archive of Earth's Oxygenation*; Melezhik, V.A., Ed.; Springer: Berlin/Heidelberg, Germany, 2013; pp. 33–38, ISBN 9783540885573.

13. Balaganskiy, V.V.; Basalayev, A.A.; Belyaev, O.A.; Pozhilenko, V.I.; Radchenko, A.T.; Radchenko, M.K. *The 1:500,000 Geological Map of the Kola Region (Northeastern Baltic Shield)*; Mitrofanov, F.P., Ed.; GI KSC RAS: Apatity, Russia, 1996. (In Russian)

14. Mitrofanov, F.P.; Zozulya, D.R.; Bayanova, T.B.; Levkovich, N.V. The world's oldest anorogenic alkali granitic magmatism in the Keivy structure on the Baltic Shield. *Dokl. Earth Sci.* **2000**, *374*, 238–241.

15. Zozulya, D.R.; Bayanova, T.B.; Eby, G.N. Geology and Age of the Late Archean Keivy Alkaline Province, Northeastern Baltic Shield. *J. Geol.* **2005**, *113*, 601–608. [CrossRef]

16. Vetrin, V.R.; Rodionov, N.V. Geology and geochronology of neoarchean anorogenic magmatism of the Keivy structure, Kola Peninsula. *Petrology* **2009**, *17*, 537–557. [CrossRef]

17. Batieva, I.D. *Petrology of Alkaline Granites in Kola Peninsula*; Nauka: Leningrad, Russia, 1976. (In Russian)

18. Balagansky, V.V.; Myskova, T.A.; Skublov, S.G. On the age of felsic metavolcanites of the Archaean Lebyazhka sequence, Kola region, Baltic Shield. In Proceedings of the Geology and Geochronology of the Rock-Forming and Ore Processes in Crystalline Shields, Apatity, Russia, 8–12 July 2013; Mitrofanov, F.P., Bayanova, T.B., Eds.; K&M Publishing House: Apatity, Russia, 2013; pp. 17–20. (In Russian)

19. Bagiński, B.; Zozulya, D.; MacDonald, R.; Kartashov, P.M.; Dzierżanowski, P. Low-temperature hydrothermal alteration of a rare-metal rich quartz–epidote metasomatite from the El'ozero deposit, Kola Peninsula, Russia. *Eur. J. Mineral.* **2016**, *28*, 789–810. [CrossRef]

20. Lyalina, L.M.; Zozulya, D.R.; Savchenko, Y.E.; Tarasov, M.P.; Selivanova, E.A.; Tarasova, E. Fluorbritholite-(Y) and yttrialite-(Y) from silexites of the Keivy alkali granites, Kola Peninsula. *Geol. Ore Depos.* **2014**, *56*, 589–602. [CrossRef]

21. Macdonald, R.; Bagiński, B.; Zozulya, D. Differing responses of zircon, chevkinite-(Ce), monazite-(Ce) and fergusonite-(Y) to hydrothermal alteration: Evidence from the Keivy alkaline province, Kola Peninsula, Russia. *Mineral. Petrol.* **2017**, *111*, 523–545. [CrossRef]

22. Bel'kov, I.V.; Batieva, I.D.; Vinogradova, G.V.; Vinogradov, A.N. *Mineralization and Fluid Regime in the Contact Zones of Alkali Granite Intrusions*; Petrov, V.P., Ed.; Academy of Sciences USSR: Apatity, Russia, 1988. (In Russian)

23. Bayanova, T.B. *Age of Reference Geological Complexes of the Kola Peninsula and Duration of the Magmatic Processes*; Nauka: St.-Petersburg, Russia, 2004. (In Russian)

24. Grew, E.S. Carbonaceous Material in Some Metamorphic Rocks of New England and Other Areas. *J. Geol.* **1974**, *82*, 50–73. [CrossRef]

25. Buseck, P.R.; Beyssac, O. From Organic Matter to Graphite: Graphitization. *Elements* **2014**, *10*, 421–426. [CrossRef]

26. Beyssac, O.; Goffé, B.; Chopin, C.; Rouzaud, J.N. Raman spectra of carbonaceous material in metasediments: A new geothermometer. *J. Metamorph. Geol.* **2002**, *20*, 859–871. [CrossRef]

27. Aoya, M.; Kouketsu, Y.; Endo, S.; Shimizu, H.; Mizukami, T.; Nakamura, D.; Wallis, S. Extending the applicability of the Raman carbonaceous-material geothermometer using data from contact metamorphic rocks. *J. Metamorph. Geol.* **2010**, *28*, 895–914. [CrossRef]

28. Lahfid, A.; Beyssac, O.; Deville, E.; Negro, F.; Chopin, C.; Goffé, B. Evolution of the Raman spectrum of carbonaceous material in low-grade metasediments of the Glarus Alps (Switzerland). *Terra Nova* **2010**, *22*, 354–360. [CrossRef]

29. Rahl, J.; Anderson, K.; Brandon, M.; Fassoulas, C. Raman spectroscopic carbonaceous material thermometry of low-grade metamorphic rocks: Calibration and application to tectonic exhumation in Crete, Greece. *Earth Planet. Sci. Lett.* **2005**, *240*, 339–354. [CrossRef]

30. Negro, F.; Beyssac, O.; Goffé, B.; Saddiqi, O.; Bouybaouene, M.L. Thermal structure of the Alboran Domain in the Rif (northern Morocco) and the Western Betics (southern Spain). Constraints from Raman spectroscopy of carbonaceous material. *J. Metamorph. Geol.* **2006**, *24*, 309–327. [CrossRef]

31. Wyhlidal, S.; Tropper, P.; Thöny, W.F.; Kaindl, R. Minor element- and carbonaceous material thermometry of high-grade metapelites from the Sauwald Zone, Southern Bohemian Massif (Upper Austria). *Mineral. Petrol.* **2009**, *97*, 61–74. [CrossRef]

32. Robert, A.; Pubellier, M.; de Sigoyer, J.; Vergne, J.; Lahfid, A.; Cattin, R.; Findling, N.; Zhu, J. Structural and thermal characters of the Longmen Shan (Sichuan, China). *Tectonophysics* **2010**, *491*, 165–173. [CrossRef]

33. Hilchie, L.J.; Jamieson, R.A. Graphite thermometry in a low-pressure contact aureole, Halifax, Nova Scotia. *Lithos* **2014**, *208–209*, 21–33. [CrossRef]

34. Long, S.P.; Gordon, S.M.; Young, J.P.; Soignard, E. Temperature and strain gradients through Lesser Himalayan rocks and across the Main Central thrust, south central Bhutan: Implications for transport-parallel stretching and inverted metamorphism. *Tectonics* **2016**, *35*, 1863–1891. [CrossRef]

35. Safonov, O.G.; Reutsky, V.N.; Varlamov, D.A.; Yapaskurt, V.O.; Golunova, M.A.; Shcherbakov, V.D.; van Reenen, D.D.; Smit, A.C.; Butvina, V.G. Composition and source of fluids in high-temperature graphite-bearing granitoids associated with granulites: Examples from the Southern Marginal Zone, Limpopo Complex, South Africa. *Gondwana Res.* **2018**, *60*, 129–152. [CrossRef]

36. Delchini, S.; Lahfid, A.; Plunder, A.; Michard, A. Applicability of the RSCM geothermometry approach in a complex tectono-metamorphic context: The Jebilet massif case study (Variscan Belt, Morocco). *Lithos* **2016**, *256–257*, 1–12. [CrossRef]

37. Luque, F.J.; Pasteris, J.D.; Wopenka, B.; Rodas, M.; Barrenechea, J.F. Natural fluid-deposited graphite: Mineralogical characteristics and mechanisms of formation. *Am. J. Sci.* **1998**, *298*, 471–498. [CrossRef]

38. Galvez, M.E.; Beyssac, O.; Martinez, I.; Benzerara, K.; Chaduteau, C.; Malvoisin, B.; Malavieille, J. Graphite formation by carbonate reduction during subduction. *Nat. Geosci.* **2013**, *6*, 473–477. [CrossRef]

39. Galimov, E.M. Isotope organic geochemistry. *Org. Geochem.* **2006**, *37*, 1200–1262. [CrossRef]

40. Reutsky, V.N.; Borzdov, Y.M.; Palyanov, Y.N. Effect of diamond growth rate on carbon isotope fractionation in Fe–Ni–C system. *Diam. Relat. Mater.* **2012**, *21*, 7–10. [CrossRef]

41. Wopenka, B.; Pasteris, J.D. Structural characterization of kerogens to granulite-facies graphite: Applicability of Raman microprobe spectroscopy. *Am. Mineral.* **1993**, *78*, 533–557.

42. Pasteris, J.D. In Situ Analysis in Geological Thin-Sections by Laser Raman Microprobe Spectroscopy: A Cautionary Note. *Appl. Spectrosc.* **1989**, *43*, 567–570. [CrossRef]

43. Beyssac, O.; Goffé, B.; Petitet, J.-P.; Froigneux, E.; Moreau, M.; Rouzaud, J.-N. On the characterization of disordered and heterogeneous carbonaceous materials by Raman spectroscopy. *Spectrochim. Acta Part A Mol. Biomol. Spectrosc.* **2003**, *59*, 2267–2276. [CrossRef]

44. Lünsdorf, N.K. Raman spectroscopy of dispersed vitrinite—Methodical aspects and correlation with reflectance. *Int. J. Coal Geol.* **2016**, *153*, 75–86. [CrossRef]

45. Tuinstra, F.; Koenig, J.L. Raman Spectrum of Graphite. *J. Chem. Phys.* **1970**, *53*, 1126–1130. [CrossRef]

46. Jaszczak, J.A.; Robinson, G.W.; Dimovski, S.; Gogotsi, Y. Naturally occurring graphite cones. *Carbon* **2003**, *41*, 2085–2092. [CrossRef]

47. Duke, E.F.; Rumble, D. Textural and isotopic variations in graphite from plutonic rocks, South-Central New Hampshire. *Contrib. Mineral. Petrol.* **1986**, *93*, 409–419. [CrossRef]

48. Barrenechea, J.F.; Luque, F.J.; Millward, D.; Ortega, L.; Beyssac, O.; Rodas, M. Graphite morphologies from the Borrowdale deposit (NW England, UK): Raman and SIMS data. *Contrib. Mineral. Petrol.* **2009**, *158*, 37–51. [CrossRef]

49. Doroshkevich, A.G.; Wall, F.; Ripp, G.S. Magmatic graphite in dolomite carbonatite at Pogranichnoe, North Transbaikalia, Russia. *Contrib. Mineral. Petrol.* **2007**, *153*, 339–353. [CrossRef]

50. Rantitsch, G.; Lämmerer, W.; Fisslthaler, E.; Mitsche, S.; Kaltenböck, H. On the discrimination of semi-graphite and graphite by Raman spectroscopy. *Int. J. Coal Geol.* **2016**, *159*, 48–56. [CrossRef]

51. Ammar, M.R.; Rouzaud, J.-N. How to obtain a reliable structural characterization of polished graphitized carbons by Raman microspectroscopy. *J. Raman Spectrosc.* **2012**, *43*, 207–211. [CrossRef]

52. Luque, F.J.; Huizenga, J.-M.; Crespo-Feo, E.; Wada, H.; Ortega, L.; Barrenechea, J.F. Vein graphite deposits: Geological settings, origin, and economic significance. *Miner. Depos.* **2014**, *49*, 261–277. [CrossRef]

53. Crespo, E.; Luque, F.J.; Barrenechea, J.F.; Rodas, M. Influence of grinding on graphite crystallinity from experimental and natural data: Implications for graphite thermometry and sample preparation. *Mineral. Mag.* **2006**, *70*, 697–707. [CrossRef]

54. Sheskin, D. *Handbook of Parametric and Nonparametric Statistical Procedures*; Chapman and Hall/CRC: New York, NY, USA, 2003; ISBN 978-1-58488-440-8.

55. Gibbons, J.; Chakraborti, S. *Nonparametric Statistical Inference. Fourth Edition, Revised and Expanded*; Marcel Dekker: New York, NY, USA, 2003; ISBN 0-8247-4052-1.

56. Hollander, M.; Wolfe, D.A. *Nonparametric Statistical Methods. Second Edition*; John Wiley & Sons: New York, NY, USA, 1999; ISBN 0-471-19045-4.

57. Sprent, P.; Smeeton, N.C.; Smeeton, N.C. *Applied Nonparametric Statistical Methods, Fourth Edition*; Chapman and Hall/CRC: New York, NY, USA, 2016; ISBN 9781439894019.

58. Bushmin, S.A.; Glebovitskii, V.A.; Prasolov, E.M.; Lokhov, K.I.; Vapnik, E.A.; Savva, E.V.; Shcheglova, T.P. Origin and composition of fluid responsible for metasomatic processes in shear zones of the Bolshie Keivy tectonic nappe, baltic shield: Carbon isotope composition of graphite. *Dokl. Earth Sci.* **2011**, *438*, 701–704. [CrossRef]

59. Sherwood Lollar, B.; Westgate, T.D.; Ward, J.A.; Slater, G.F.; Lacrampe-Couloume, G. Abiogenic formation of alkanes in the Earth's crust as a minor source for global hydrocarbon reservoirs. *Nature* **2002**, *416*, 522–524. [CrossRef]

60. Lollar, B.S.; Lacrampe-Couloume, G.; Voglesonger, K.; Onstott, T.C.; Pratt, L.M.; Slater, G.F. Isotopic signatures of CH_4 and higher hydrocarbon gases from Precambrian Shield sites: A model for abiogenic polymerization of hydrocarbons. *Geochim. Cosmochim. Acta* **2008**, *72*, 4778–4795. [CrossRef]

61. Sherwood Lollar, B.; Frape, S.K.; Weise, S.M.; Fritz, P.; Macko, S.A.; Welhan, J.A. Abiogenic methanogenesis in crystalline rocks. *Geochim. Cosmochim. Acta* **1993**, *57*, 5087–5097. [CrossRef]

62. Sherwood, B.; Fritz, P.; Frape, S.K.; Macko, S.A.; Weise, S.M.; Welhan, J.A. Methane occurrences in the Canadian Shield. *Chem. Geol.* **1988**, *71*, 223–236. [CrossRef]

63. Stahl, W. Carbon isotope fractionations in natural gases. *Nature* **1974**, *251*, 134–135. [CrossRef]

64. Ni, Y.; Dai, J. Geochemical characteristics of abiogenic alkane gases. *Pet. Sci.* **2009**, *6*, 327–338. [CrossRef]

65. Cai, C.; Zhang, C.; Worden, R.H.; Wang, T.; Li, H.; Jiang, L.; Huang, S.; Zhang, B. Application of sulfur and carbon isotopes to oil–source rock correlation: A case study from the Tazhong area, Tarim Basin, China. *Org. Geochem.* **2015**, *83–84*, 140–152. [CrossRef]

66. Shen, P.; Xu, Y.C. A study of carbon isotopes from oils. *Chin. Sci. Bull.* **1998**, *43*, 117. [CrossRef]

67. Astafieva, M.M.; Balaganskii, V.V. Keivy Paraschists (Archean–Early Proterozoic): Nanobacteria and Life. *Stratigr. Geol. Correl.* **2018**, *26*, 354–363. [CrossRef]

68. Kozlov, N.E.; Sorokhtin, N.O.; Martynov, E.V. Geodynamic Evolution and Metallogeny of Archaean Structural and Compositional Complexes in the Northwestern Russian Arctic. *Minerals* **2018**, *8*, 573. [CrossRef]

69. Luque, F.J.; Crespo-Feo, E.; Barrenechea, J.F.; Ortega, L. Carbon isotopes of graphite: Implications on fluid history. *Geosci. Front.* **2012**, *3*, 197–207. [CrossRef]

70. Santosh, M.; Wada, H. A Carbon Isotope Study of Graphites from the Kerala Khondalite Belt, Southern India: Evidence for CO_2 Infiltration in Granulites. *J. Geol.* **1993**, *101*, 643–651. [CrossRef]

71. Baiju, K.R.; Nambiar, C.G.; Jadhav, G.N.; Kagi, H.; Satish-Kumar, M. Low-density CO_2-rich fluid inclusions from charnockites of southwestern Madurai Granulite Block, southern India; implications on graphite mineralization. *J. Asian Earth Sci.* **2009**, *36*, 332–340. [CrossRef]